Polymer Bulletin
https://doi.org/10.1007/s00289-024-05188-y

ORIGINAL PAPER

Agar aerogel powder particles for future life science applications: fabrication and investigations on swelling behavior and cell compatibility

Claudia Keil[1] · Anja Hajnal[2] · Julia Keitel[1] · Helena Kieserling[3] · Sascha Rohn[3] · Tamara Athamneh[4] · Hajo Haase[1] · Pavel Gurikov[2,5]

Received: 9 October 2023 / Revised: 2 February 2024 / Accepted: 2 February 2024

Abstract

The use of bio-based raw materials in the manufacture of customized aerogels has increased significantly over the last decade. Combining the advantages of biopolymer sustainability and lower costs when producing aerogels in particulate form, agar aerogel particles were fabricated in this study. They were prepared by successive thermal gelation, ethanol solvent exchange, wet milling and supercritical CO_2 assisted drying. The particles still maintain high porosity (~ 1.0 $cm^3\ g^{-1}$) and high specific surface areas (210–270 $m^2\ g^{-1}$). The stability in wound fluid substitutes, liquid holding capacity, and cytocompatibility of these agar-based aerogel particles may make them an advantageous wound-dressing matrix that can be further customized for particular applications by adding wound-active/reactive substances, such as antibiotics, antioxidants, immunoreactive drugs or growth factors.

Claudia Keil and Anja Hajnal have contributed equally.

✉ Claudia Keil
c.keil@tu-berlin.de

✉ Pavel Gurikov
pavel.gurikov@tuhh.de

[1] Department of Food Chemistry and Toxicology, Institute of Food Technology and Food Chemistry, Technische Universität Berlin, Straße des 17. Juni 135, 10623 Berlin, Germany

[2] Laboratory for Development and Modelling of Novel Nanoporous Materials, Hamburg University of Technology, Eißendorfer Straße 38, 21073 Hamburg, Germany

[3] Department of Food Chemistry and Analysis, Institute of Food Technology and Food Chemistry, Technische Universität Berlin, Straße des 17. Juni 135, 10623 Berlin, Germany

[4] Institute of Nanotechnology, Jordan University of Science and Technology, Irbid 22110, Jordan

[5] Aerogel-It GmbH, Albert-Einstein-Str. 1, 49076 Osnabrück, Germany

Published online: 28 February 2024

Graphical abstract

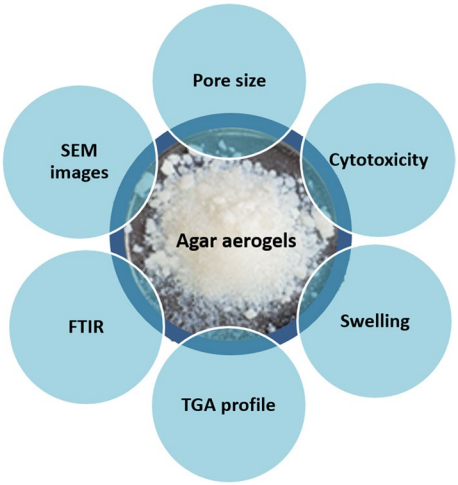

Keywords Aerogel · Agar · Biopolymer · Supercritical CO_2 · Wound dressing

Introduction

The life sciences and biotechnology sector has been facing the challenge of addressing the environmental and sustainability agenda for many years now. The sector aims to ensure resource efficiency through energy efficiency and circular economy and to address renewable resources, which include both natural biopolymers and chemically synthesized molecules from biological materials [1–3]. Due to their biodegradable properties and biocompatibility, biopolymers are useful for a variety of life science applications, including edible films, emulsions, packaging materials in the food industry, drug delivery materials, medical implants, wound healing, tissue scaffolds, and dressing materials in the pharmaceutical industry [4–6]. Creating porous, three-dimensional, ultra-light aerogel materials further expands the potential applications of biopolymers in the life science sector [7–12]. Since the invention of aerogels in 1931 by Steven Kistler [13], aerogels made from bio-based materials have been highly valued in research and applications. To realize their full potential, advanced strategies need to be developed, to shorten production times and reduce costs so that bio-aerogel production can transit from laboratory phase to commercial scale [14–18]. Aerogels containing polysaccharides account for most of the current bio-applications [17, 19].

In recent decades, a variety of natural raw materials and their combinations [17, 20, 21] along with various preparation technologies (e.g., covalent, ionic, pH-induced, thermal or cryo-cross-linking) have been investigated to develop polysaccharide-based aerogels with different functions for diverse applications [16, 22]. In addition, polysaccharide-based aerogels can be also tailored for intended

use by fabricating them in different forms such as monoliths, films, beads, particles, fibers, or scaffolds [7, 20, 23–25].

Aerogel particles, in particular, bring advantages when it comes to processing, as they need shorter solvent exchange and extraction times [12]. They can be produced by several different methods based on droplet generation from biopolymer solutions, such as the conventional dropping method, vibrating nozzle, electrostatic method, mechanical cutting, spraying, and the formation of spherical droplets in an oil phase [16]. Alternatively, particles can also be produced by downmilling of larger hydro-, alco- or aerogel structures. Depending on the method used, aerogel particles can be of different sphericities and sizes [26]. This form of aerogels serves a wide range of applications. They are used for insulation purposes or in life science fields as sorption material or carriers for flavors, drugs, and cosmetic ingredients [16].

Agar is a polysaccharide that has been widely used in life sciences, most commonly food, cosmetics, pharmaceutical, and biotechnology sectors [27]. Aerogels from this precursor were mentioned as early as in the work of Kistler [13], but have since rarely been reported in the literature in this context. Agar is a natural hydrophilic polymeric polysaccharide extracted from the cell of red algae and consists of two polymers, agarose and agaropectin. Agarose is a disaccharide made up of D-galactose and 3,6-anhydro-L-galactopyranose, while agaropectin is a mixture of smaller molecules made of alternating units of D-galactose and L-galactose modified with acidic side groups [28]. Agar demonstrates high gelling ability, mainly due to the agarose component, forming strong gels at a broad range of polymer concentrations [29]. Furthermore, the previous works demonstrated that aerogel slabs, tablets and beads can be produced from this polysaccharide with reasonable quality via the supercritical drying route reaching surface areas of up to 320 m^2/g [23, 30–32]. Agar aerogel tablets have also been demonstrated to be a promising material for wound dressing applications in an in vivo study. The results suggested easy removal from the wound site, complete healing of the skin and shorter healing time compared to that of gauze-treated wounds [32]. However, additional properties need to be evaluated to complement these findings and support further biomedical applications of agar aerogels.

The aim of this work was to produce sustainable agar aerogels in particulate form and characterize their physico-chemical properties, swelling capacity and biocompatibility. Wet-milling method, followed by a supercritical CO_2 (sc-CO_2)-assisted "green processing technology" combining material performance, environmental and safety aspects [33] was applied. The physico-chemical characterization of the aerogels was done by nitrogen sorption analysis, Fourier transform infrared spectroscopy (FTIR), thermogravimetric analysis (TGA) and high-resolution scanning electron microscopy (HR-SEM). With regard to the possible use of these materials as liquid absorbers, the preservation of the porous aerogel scaffold structure is important. Therefore, the free swelling capacity (FSC) and centrifuge retention capacity (CRC) of the aerogels were determined using distilled water, PBS buffer or simulated body fluid as aqueous medium. Finally, the cell compatibility of the synthesized aerogels was investigated on a range of mammalian cells.

Materials and methods

Materials

Agar (extracted red alga/ Rhodophyceae), $CaCl_2$, $CaCO_3$, DMSO, ethanol, K_2HPO_4, 3-(4,5-Dimethylthiazol-2-yl)-2,5-diphenyl-tetrazolium bromide (MTT), $MgCl_2$, NaCl, NaH_2PO_4, $NaHCO_3$ and Na_2SO_4, were purchased from Carl Roth GmbH + Co. KG (Karlsruhe, Germany). Cell Counting Kit-8/water soluble tetrazolium (WST)-8, D-(+)-gluconic acid δ-lactone (GDL), ethylenediaminetetraacetic acid (EDTA), (4-(2-hydroxyethyl)-1-piperazineethanesulfonic acid (HEPES), KCl, penicillin–streptomycin, Sodium alginate (derived from brown seaweeds/ Phaeophyceae), Triton-X-100 were delivered from Sigma-Aldrich Chemie GmbH (Taufkirchen, Germany). CO_2 (purity > 99%) was obtained from Praxair GmbH (Ratingen, Germany). Dulbecco's Modified Eagles Medium (DMEM) and fetal calf serum (FCS) were from PAN-Biotech (Aidenbach, Germany).

Aerogel preparation

Agar hydrogels (0.5, 1.0, 2.0 or 3.0% w/w) were prepared as described by Tetsujiro Matsuhashi [34] by heating water to 95 °C using a water bath and subsequent addition of the appropriate mass of the agar powder. The solutions were covered and stirred continuously for 1 h to completely dissolve the agar, after which hot agar/water solutions are poured into the molds (polystyrene 6-well plates) and left at room temperature to gel into hydrogel discs with a diameter of 30 mm and a height of ~ 5 mm. Prior to the solvent exchange, the agar hydrogels were removed from the molds. The solvent exchange was done by immersing the hydrogels in the excess of pure ethanol. This was repeated several times to ensure the complete removal of water from the gels. For each solvent exchange step, the gels were left in ethanol overnight (~ 15 h) to allow for the mass transfer between the gels and the bulk to be completed. The agar alcogels were crushed in a blender (SM 3718, Severin) to a particle size of about 1 mm and subsequently ground in a colloid mill (IKA magic LAB; Grinding speed: 2200 rpm; Mill gap: 900 µm). The obtained alcogel particles were packed in filter paper bags and dried under constant CO_2 influx for ~ 8 h at 60 °C and 120 bar as described by Gurikov et al. [35].

Textural properties of aerogels

Images of agar aerogel particles were taken by light microscopy (VisiScope TL384H). Nitrogen adsorption–desorption analysis (Quantachrome Nova 3000e) was used to determine the microstructural properties of the agar aerogel powders. The specific surface area (S_{BET}) was determined by Brunauer–Emmett–Teller (BET) method and the pore size distribution, mesopore radius ($r_{mesopore}$) and mesopore volume ($V_{mesopore}$) were estimated by Barrett–Joyner–Halenda (BJH) method.

All samples were degassed under vacuum at 60 °C for at least 6 h prior to the measurements.

SEM pictures were recorded on a Field Emission Scanning Electron Microscope Zeiss DSM 982 GEMINI equipped with a secondary electron in-lens detector (Carl Zeiss Microscopy GmbH, Jena, Germany) and the DISS6 acquisition software (point electronic GmbH, Halle/Saale, Germany) after sputtering with gold (6 nm gold coating, Baltec Sputter Coater SCD 050). Measurements were carried out at an accelerating voltage of 6 kV and under high vacuum.

FTIR analysis

Infrared spectra of the aerogel material were measured with a Bruker Tensor II spectrometer (Bruker Optic GmbH, Karlsruhe, Germany) equipped with a liquid nitrogen-cooled mercury-cadmium-telluride detector. The samples were measured in absorption mode with a Platinum ATR Diamond cell (Bruker Optic GmbH, Karlsruhe, Germany) against air as background. Each spectrum results from an average of 120 scans recorded with a resolution of 2 cm^{-1} from 4,000 to 800 cm^{-1} at 20 °C. Spectra were off set-corrected in the region of 3,800–4,000 cm^{-1} using the software provided with the spectrometer (OPUS 7.5). The peaks were normalized to the highest intensity values.

Swelling properties

Swelling studies were done using either distilled water, PBS buffer (137 mM NaCl; 2.7 mM KCl; 2 mM Na_2HPO_4; 1.8 mM KH_2PO_4); PBS + 1 M NaCl or simulated body fluid (SBF) (137 mM NaCl; 4.1 mM $NaHCO_3$; 3 mM KCl; 0.1 mM K_2HPO_4; 1.5 mM $MgCl_2$; 2.5 mM $CaCl_2$; 0.5 mM Na_2SO_4; 50 mM Tris; 45 mM HCl; pH 7.4) [36] as liquids with free swelling capacity and centrifuge retention capacity methodology.

The free swelling capacity is commonly referred to as the "teabag method" [37]. Empty tea bags (paper filters, size M: 23 × 110 × 146 mm) of defined weight were filled with defined quantities of aerogel material (~ 50 mg) and soaked in beakers each containing 1 L of the swelling solutions at either 25 °C or 50 °C. The swollen tea bags were removed from the beakers after 24 h, a previously established time frame sufficient for achieving maximum swelling of powdered aerogels in human body fluid-like liquids [38]. Excess moisture on the tea bag surface was then absorbed using filter paper and the weight of the tea bags was determined immediately. Empty teabags ($N = 3$) went through the same steps to serve as controls. Based on the determined weights, the free swelling capacity (FSC) was calculated according to the following equation:

$$\mathrm{FSC}\left[g_{\mathrm{liquid}}/g_{\mathrm{aerogel}}\right] = \frac{m_s - (m_{\mathrm{empty\ wet\ teabag}} + m_0)}{m_0} \quad (1)$$

with $m_0 \triangleq$ initial weight of dry aerogel; $m_s \triangleq$ weight of the swollen aerogel-teabag sample; $m_{\text{empty wet bag}} \triangleq$ weight of the swollen empty teabag.

The centrifuge retention capacity refers to the ability of aerogels to retain fluids after being saturated and centrifuged under controlled conditions [39]. Briefly, aerogels were incubated at a final concentration of 10 mg/mL in reaction tubes for 24 h at either 25 or 50 °C (Thermomixer 5436, Eppendorf SE, Hamburg, Germany), then dehydrated for 5 min by 300 g (Heraeus Fresco 17, Heraeus Holding GmbH, Hanau, Germany) and reweighed. Centrifuge Retention Capacity (CRC) was calculated according to the following equation:

$$\text{CRC}\left[g_{\text{liquid}}/g_{\text{aerogel}}\right] = \frac{m_s - (m_{\text{empty tube}} + m_0)}{m_0} \tag{2}$$

with $m_0 \triangleq$ initial weight of dry aerogel; $m_s \triangleq =$ weight of the swollen tube-aerogel sample; $m_{\text{empty tube}} \triangleq$ weight of the empty tube before adding the aerogel.

Cell culture studies

Mouse NIH-3T3 fibroblasts [40], HaCat immortalized human keratinocytes [41] and the human spontaneously immortalized monocyte-like THP-1 cells [42] are available from the American Type Culture Collection (ATCC; Manassas, Virginia). Cells were cultured in Dulbecco's Modified Eagle Medium (DMEM) containing 10% FCS (heat inactivated for 30 min at 56 °C), 2 mM L-glutamine, 100 µg/ml potassium penicillin, and 100 µg/ml streptomycin. Cells were maintained in 75 cm^2 culture flasks, subcultured three times a week (seeding 30,000 cells/cm^2) and incubated at 37 °C in a 5% CO_2 humidified atmosphere. Adherent cells were detached when confluence reached about 80% using 0.25% trypsin/EDTA at 37 °C. The cells were collected in DMEM and cell number and viability were determined using a CASY® Model TT cell counter (OMNI Life Science GmbH & Co. KG, Bremen, Germany). The viability of the cells after contact with the aerogels was evaluated using the MTT and CCK-8 cytotoxicity assays [43], both based on the metabolic conversion of tetrazolium dyes into formazans, which are used as indicators of cell viability [44]. Cells were seeded in 24-well plates at a density of 30.000 cells/ml $DMEM_{\text{without phenolred}}$ and maintained in culture for 24 h (~1 doubling period) to form semi-confluent monolayers. THP-1 monocytes were pretreated with phorbol 12-myristate 13-acetate (5 ng PMA/ml) for differentiation into macrophage-like cells [45]. Following a 72 h incubation period in the presence of the aerogel dispersions (1–2.5 mg_{aerogel}/ml $DMEM_{\text{without phenolred}}$) or medium as a control, cell viability was analyzed incubating either with the water soluble tetrazolium salt CCK-8 (diluted 1:20) (WST-8 assay) or 0.5 mg/mL 3-(4,5-Dimethylthiazol-2-yl)-2,5- diphenyltetrazolium bromide (MTT). In case of the MTT-assay cells were lysed by adding 500 µl of a 1:1 mixture of pure ethanol and DMSO. The absorption was determined on a well plate reader (M200, Tecan, Swiss) at 450 nm (WST) or 570 nm (MTT). Incubations with aerogel-untreated cells were included to define the maximum metabolic activity (100% control). The positive control of cytotoxicity was achieved by treatment with 0.1% v/v Triton-X-100 solution diluted in $DMEM_{\text{without phenolred}}$, causing around 92% (MTT

assay) or 86.5% (CCK-8 assay) cytotoxicity. Calcium-crosslinked alginate aerogels were also studied in cytotoxicity tests on NIH-3T3 fibroblasts and macrophage-like THP-1 cells (see Supplementary Material for details).

Statistical analyses

Statistical significance of experimental results was calculated by GraphPad prism software version 8.02 (GraphPad Software Inc., CA, USA) using the tests indicated in the respective figure legends.

Results and discussion

Fabrication process of agar aerogel powder particles

Agar alcogels obtained from 0.5 to 3.0 wt.% solutions were all successfully down-milled into particles. In the case of lower agar concentrations of 0.5 and 1 wt.%, the particles agglomerated, forming compacts during the drying so that loose powder could not be obtained (data not shown). At lower polymer concentration during agar gelation, pore size becomes larger and polymer chains more loosely packed [46]. As the mechanical properties of biopolymer aerogels scales with their density [47, 48], samples obtained at lower agar concentrations are softer, resulting in their deformation during drying. In contrast, alcogels from 2 to 3 wt.% solutions were successfully dried; agar aerogel particles were obtained and used in further analyses. The light microscopy images of particles (Fig. 1A, B) show that they have low sphericity and roundness with up to several hundred micrometers in size. In both corresponding powders (Fig. 1C, D), and more so in 2 wt.% powder, some agglomeration of agar aerogel particles is present due to the entanglement of soft particles and electrostatic attractions.

Characterization of the agar aerogel powder particles

The measured BET specific surface area of agar aerogel powders, as shown in Table 1, is fairly high, but systematically lower than for monolithic aerogels prepared from the same starting material and by the same supercritical drying route [32].

There is a possibility that the shear forces that occur during wet milling might have an effect on the network of soft agar gel, although the literature on wet milling of alginate gels reports an increase of the mesopore volume and narrowing of pore size distributions [26]. The BJH pore size distribution (Fig. 2A) shows that a small volume of mesopores is present in the sample (1.0–1.2 $cm^3\ g^{-1}$), which is in accordance with previous observations on agar aerogels [32, 49]. This is further confirmed in the SEM images of 2 and 3 wt.% agar aerogel particles (Fig. 2B) that reveal their fibrillar open porous structure.

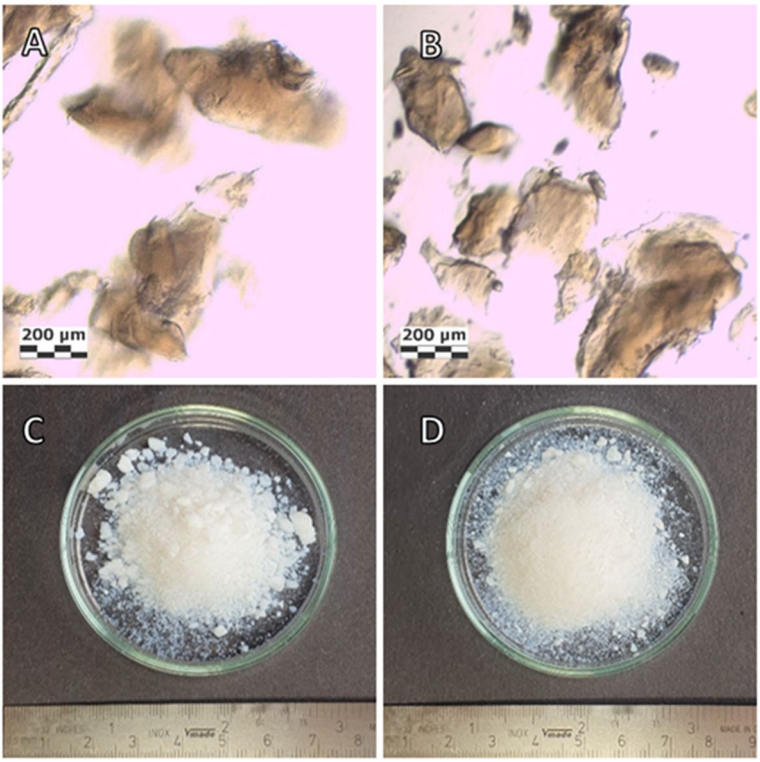

Fig. 1 Light microscopic images of the agar aerogel particles made from 2 (**A**) and 3 wt.% solutions (**B**). Photographs of the corresponding agar aerogel powders from 2 wt.% (**C**) and 3 wt.% (**D**) solutions

Table 1 Textural data for agar aerogel particles derived from 2 and 3 wt.% solutions

w_{agar} (%)	S_{BET} (m^2g^{-1})	$V_{mesopore}$ (cm^3g^{-1})	$r_{mesopore}$ (nm)
2	264	1.0	8.5
3	212	1.2	8.3

The FTIR spectra of pristine agar and agar aerogel powders are presented in Fig. 3, and all identified absorption bands are summarized in Table 2 [50–52]. All the functional groups present in the starting material could also be identified in the aerogel powders indicating that the chemical structure has not changed due to aerogel processing.

Thermogravimetric analysis (TGA) was performed to measure low-temperature water loses and high-temperature stability (Fig. 4). Being highly porous materials, aerogels may contain a substantial amount of residual solvent [53]. From our experience, biopolymer-based aerogels, which are properly dried with sc-CO_2, demonstrate up to 10–20 wt.% weight loss when degassed for the nitrogen porosimetry.

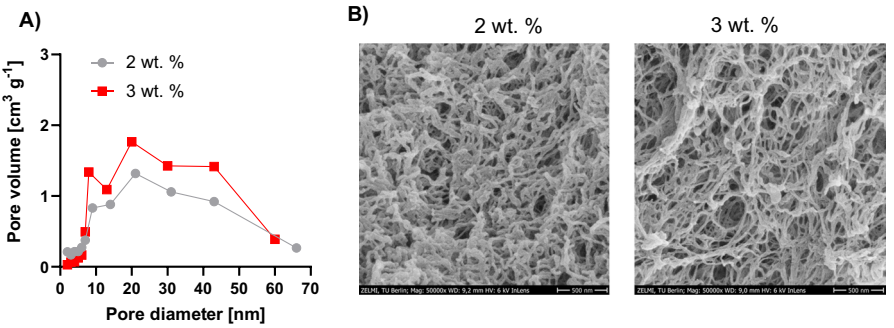

Fig. 2 **A** BJH pore size distribution and **B** SEM image of agar aerogel derived from 2 and 3 wt.% solutions

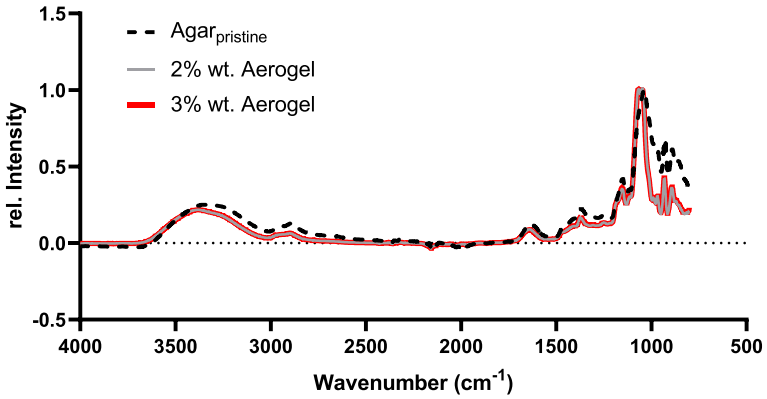

Fig. 3 Fourier transform infrared spectroscopy (FTIR) spectra of agar and agar-based aerogels with 2 and 3 wt.%. Shown are relative signal intensities normalized to the highest intensity values

Table 2 List of FTIR signal assignments of agar and agar-based aerogels

Wavenumbers (cm^{-1})	Groups/Bonds
3400	Hydroxyl group (–OH)
2900	Methoxy group (O–CH_3)
1640	Acetone group (C = O), Amide I
1370	Sulfate group (O = S = O)
1150	Ether-sulfate links
1045–1065	C–O and C–C stretching, C–O–H bending
930	C–O–C bond vibration of 3,6-anhydro-L-galactose
890	Vibration mode of β-D-galactopyranosyl residues

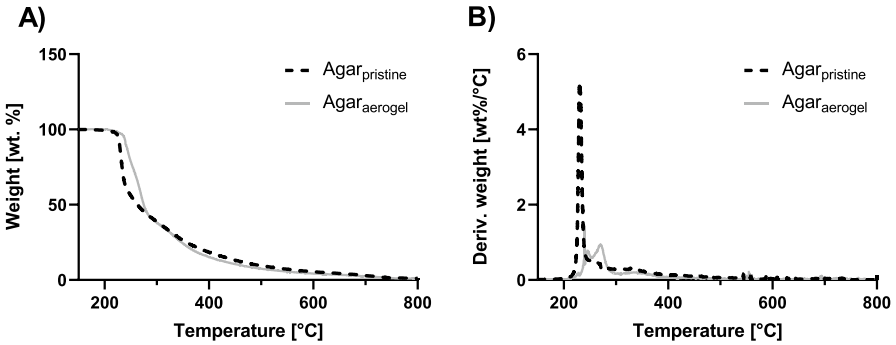

Fig. 4 **A** Weight lost of 2 wt.% agar aerogel and pristine agar powder and **B** the first derivative of the TGA profile with respect to temperature

Literature values for metal-crosslinked alginate aerogels have been determined in a similar range (8–23%), see refs. [54, 55]. The agar aerogels reported here lose ~ 12 wt.% upon heat to 150 °C, comparable to the pristine agar powder (ca. 14 wt.%), data not shown. These values are very similar to the recent results on alginate [56] and chitosan aerogels [57]. Above 150 °C, the thermal degradation profiles are very similar for aerogel and starting agar powder, when judged by TGA profiles (Fig. 4a). The first derivative of the TGA profile suggests a complex degradation mechanism of agar aerogels with multiple thermal events when compared to the pristine powder (Fig. 4b). Such a complex behavior is known for other biopolymer-based aerogels [57], but comparisons between the starting polymer and the corresponding aerogels are rarely performed. Available TGA data points to a rather polymer-specific behavior with only minor differences in TGA profiles for agarose aerogels and starting powder [31], and more pronounced differences for cellulose [58]. The latter can be associated with loss of crystallinity when cellulose is processed into an aerogel [58].

Same as previous studies [36, 38], swelling of the bio-aerogels was performed in phosphate buffer and high salinity solutions, simulated plasma body fluids and water as wound fluid-like swelling agents (Fig. 5). Because agar is sparingly soluble in cold water, the effect of temperature on the fluid uptake was studied at room temperature (25 °C) and elevated temperature (50 °C). In wound treatments, local hyperthermia (41–43 °C) can promote cell proliferation, angiogenesis, healing, and bone growth. The use of hyperthermia (above 50 °C) to treat infected wounds can stop the proliferation of bacteria [59]. Several studies have been conducted in recent years in which photothermal hydro- and aerogels have been investigated [60–62]. Furthermore, the effect of temperature on swelling has never been studied for aerogels, to the best of our knowledge, and has only rarely been reported for biopolymer-based hydrogels [63]. As shown in the following, the temperature highly affects aerogel hydration for some fluids and the obtained data may be of interest for a broad application of aerogels in the life science domain.

Based on the quantitative assessment of fluid uptake, it was concluded that the free swelling capacity for both 2 and 3 wt.% agar aerogels and for all tested media and temperatures is lower than the centrifuge retention capacity (Fig. 6A–D).

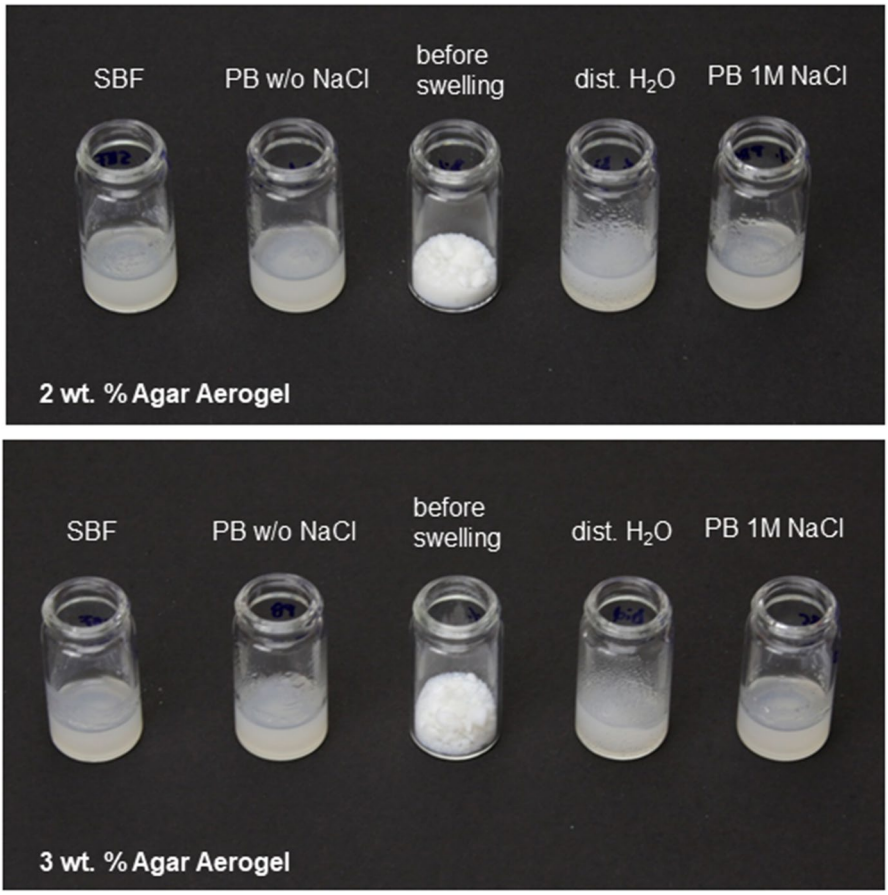

Fig. 5 Photographs of Agar-based aerogel particles before and after swelling for 24 h at 25 °C

Free fluid uptake of aerogels is apparently a multi-step process wherein mass transfer through the porous network, relaxation of the primary fibers and individual polymer chains take place at different time scales [64]. The fluid uptake process has also a spatial dimension: it seems that a thin hydrogel layer is quickly formed on the aerogel surface upon contacting liquid medium. The liquid then has to propagate through a progressively growing layer of hydrogel [64]. The hydrogel further swells in the course of the fluid uptake, compressing adjacent pores of still medium-free aerogel and thus slowing down the liquid penetration. On the contrary, when the centrifuge retention capacity is measured, the mass transfer can be enhanced by centrifugal forces [65]. These phenomena (all deserve a dedicated study) may be a plausible explanation for the fact that the free swelling capacity did not reach the water content of the starting hydrogel, 98/2 and 97/3 (mass water per mass of agar), or 49.0 and 32.3 $g_{water}/g_{hydrogel\ solution}$, for 2 and 3 wt.% agar, respectively. In contrast, the values of the centrifuge retention capacity

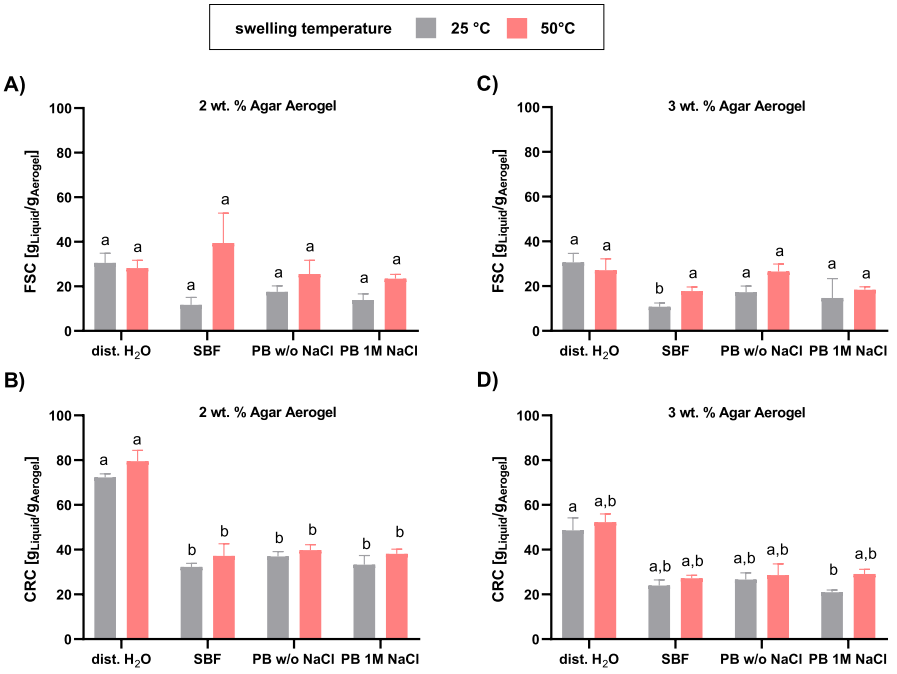

Fig. 6 Swelling capacity of the Agar-based aerogel particles. Free swelling capacity (FSC) (A/C) and the centrifuge retention capacity (CRC) (B/D) of aerogel particles following 24 h treatment with either distilled water, PBS buffer without NaCl, PBS + 1 M NaCl or simulated body fluid (SBF)). Data are presented as means ± standard error of the mean of three independently performed replicates. Bars with the same letters are not significantly different (Two-way ANOVA with Tukey's post-hoc test, $p < 0.05$)

are close to the water content in the starting hydrogels and exceed it for distilled water. In the latter case, a more swollen state than the pristine hydrogel is apparently formed.

Biocompatibility of the agar aerogel powder particles

Metabolic activity assays were carried out to explore the biocompatibility of the aerogels. The cell viability of human HaCat keratinocytes cells after treatment with immersed solutions of alginate- or agar-based aerogels was evaluated with MTT-and WST-8 tests [43, 44].

As shown in Fig. 7, the aerogels proved to be biocompatible for the immortalized human keratinocytes. There was some loss of metabolically activity for the NIH-3T3 fibroblasts and the macrophage-like THP-1 cells compared to control-treatments (see Suppl Fig. 1). Still, the intermolecular interactions between the agar aerogel matrix and wound healing cells in the local skin environment need to be studied in greater depth in the future, for which ex-vivo human skin [66, 67] is probably the best preclinical model.

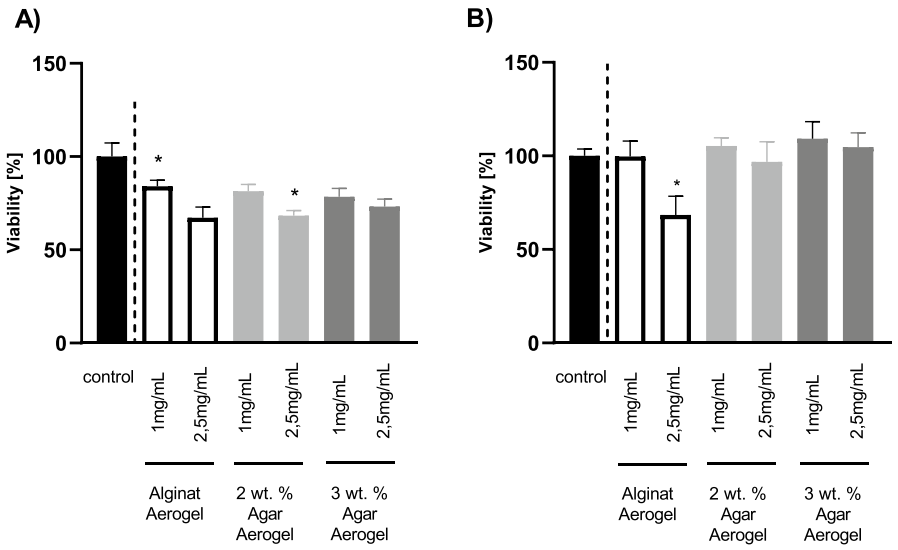

Fig. 7 HaCat cytotoxicity test results. HaCat fibroblasts were seeded into cell culture microtiter-plates and treated with aerogel dispersions for 72 h. A HaCat cell series without particulate aerogels served as a reference control. Subsequently, the metabolic activity of the cells was determined with an MTT (**A**) or WST-8 (**B**) metabolic activity assay. Data are presented as means ± standard error of the mean of three independently performed replicates. Significant differences to control are indicated (One-way ANOVA with a Dunnett's post-hoc test, *$p < 0.05$)

Conclusion

Porous biomaterials have gained a lot of attention in biomedical research and applications. In the current study, particulate agar-based aerogels were prepared and evaluated as a novel wound dressing material. There are many advantages to the particulate agar aerogels, including a relatively fast and inexpensive production and structural advantages, such as mesoporosity and high specific surface area that facilitate wound fluid absorption and rapid transfer into an aerogel network. Biocompatibility tests of the agar aerogels are promising, but further tests in 2D/3D skin cell cultures or ex-vivo skin models are needed before preclinical testing on animals or humans. The healing of a wound is a complex process involving biochemical factors and mechanical forces. Enhancing the properties of porous biopolymer gels with regard to these parameters is a challenge, but also a step in the direction of improved functional wound dressing materials.

Supplementary Information The online version contains supplementary material available at https://doi.org/10.1007/s00289-024-05188-y.

Acknowledgements We thank Christoph Fahrenson from the Center for Electron Microscopy (ZELMI), Technische Universität Berlin for carrying out the SEM investigations. We also thank Silvia Heim for conducting FT-IR analysis.

Author contributions Conceptualization: [CK, PG]; project administration: [CK, PG]; Supervision: [CK]; Data curation: [CK, AH]; formal analysis: [CK, AH]; Investigation: [CK, AH, JK, HK]; funding

acquisition: [PG]; Resources: [PG, SR, HH]; writing—original draft: [CK, AH, PG]; writing—review and editing: [CK, AH, HK, TA, SR, HH, PG]. All authors read and approved the final manuscript.

Funding Open Access funding enabled and organized by Projekt DEAL. P.G. and A.H. gratefully acknowledge support for this research from the German Research Foundation (DFG) under the Project GU 1842/3–1. Publishing fees supported by Funding Programme Open Access Publishing of Hamburg University of Technology (TUHH).

Declarations

Conflict of interest The authors declare no conflict of interest.

References

1. Sun Y, Bai Y, Yang W, Bu K, Tanveer SK, Hai J (2022) Global trends in natural biopolymers in the 21st century: a scientometric review. Front Chem 10:1–17
2. Samir A, Ashour FH, Hakim AAA, Bassyouni M (2022) Recent advances in biodegradable polymers for sustainable applications. Npj Mater Degrad 6(1):68
3. Hussein FH, Yahya FAK (2020) Biopolymers, biocomposites, and their types. In: Ahmed S (ed) Advanced green materials: fabrication, characterization and applications of biopolymers and biocomposites. Woodhead Publishing in Materials, Sawston, pp 43–60
4. Suarato G, Bertorelli R, Athanassiou A (2018) Borrowing from nature: biopolymers and biocomposites as smart wound care materials. Front Bioeng Biotechnol 6:1–11
5. Baranwal J, Barse B, Fais A, Delogu GL, Kumar A (2022) Biopolymer: a sustainable material for food and medical applications. Polymers (Basel) 14(5):1–22
6. Biswas S, Pal A (2021) Application of biopolymers as a new age sustainable material for surfactant adsorption: a brief review. Carbohydr Polym Technol Appl 2:100145
7. García-González CA, Sosnik A, Kalmár J, De Marco I, Erkey C, Concheiro A et al (2020) Aerogels in drug delivery: from design to application. J Control Release 2021(332):40–63
8. Anton-Sales I, Roig-Sanchez S, Sánchez-Guisado MJ, Laromaine A, Roig A (2020) Bacterial nanocellulose and titania hybrids: cytocompatible and cryopreservable cell carriers. ACS Biomater Sci Eng 6(9):4893–4902
9. Bernardes BG, Del Gaudio P, Alves P, Costa R, García-Gonzaléz CA, Oliveira AL (2021) Bioaerogels: promising nanostructured materials in fluid management, healing and regeneration of wounds. Molecules 26(13):3834
10. Manzocco L, Mikkonen KS, García-González CA (2021) Aerogels as porous structures for food applications: smart ingredients and novel packaging materials. Food Struct 28:100188
11. Feng J, Su BL, Xia H, Zhao S, Gao C, Wang L et al (2021) Printed aerogels: chemistry, processing, and applications. Chem Soc Rev 50(6):3842–3888
12. Smirnova I, Gurikov P (2017) Aerogels in chemical engineering: strategies toward tailor-made aerogels. Annu Rev Chem Biomol Eng 8:307–334
13. Kistler SS (1931) Coherent expanded aerogels and jellie. Nature 127(3211):3211

14. Maleki H, Durães L, García-González CA, del Gaudio P, Portugal A, Mahmoudi M (2016) Synthesis and biomedical applications of aerogels: possibilities and challenges. Adv Colloid Interface Sci 236:1–27
15. Smirnova I, Gurikov P (2018) Aerogel production: current status, research directions, and future opportunities. J Supercrit Fluids 134:228–233
16. Ganesan K, Budtova T, Ratke L, Gurikov P, Baudron V, Preibisch I et al (2018) Review on the production of polysaccharide aerogel particles. Materials (Basel) 11(11):1–37
17. Nita LE, Ghilan A, Rusu AG, Neamtu I, Chiriac AP (2020) New trends in bio-based aerogels. Pharmaceutics 12(5):449
18. Djati Utomo H, Li X, Ng ETJ (2022) Sustainable production in circular economy: aerogel upscaling production. Environ Sci Pollut Res 29(14):20078–20084
19. Zhao S, Malfait WJ, Guerrero-Alburquerque N, Koebel MM, Nyström G (2018) Biopolymer aerogels and foams: chemistry, properties, and applications. Angew Chemie Int Ed 57(26):7580–7608
20. Muhammad A, Lee D, Shin Y, Park J (2021) Recent progress in polysaccharide aerogels: their synthesis, application, and future outlook. Polymers (Basel) 13:1347
21. Gaggero G, Subrahmanyam RP, Schroeter B, Gurikov P, Delucchi M (2022) Organic bio-based aerogel from food waste: preparation and hydrophobization. Gels 8:691
22. Wang Y, Su Y, Wang W, Fang Y, Riffat SB, Jiang F (2019) The advances of polysaccharide-based aerogels: preparation and potential application. Carbohydr Polym 226:115242
23. Robitzer M, Di Renzo F, Quignard F (2011) Natural materials with high surface area. Physisorption methods for the characterization of the texture and surface of polysaccharide aerogels. Microporous Mesoporous Mater 140(1–3):9–16
24. Stergar J, Maver U (2016) Review of aerogel-based materials in biomedical applications. J Sol-Gel Sci Technol 77(3):738–752
25. Sonu SS, Rai N, Chauhan I (2023) Multifunctional aerogels: a comprehensive review on types, synthesis and applications of aerogels. J Sol-Gel Sci Technol 105(2):324–336
26. Schroeter B, Jeansathawong P, Hajnal A, Gurikov P (2023) Wet milling of alginate alco- and hydrogel composites: a facile top-down approach for continuous production of aerogel microparticles. Macromol Mater Eng 308:2200674
27. Sousa AMM, Rocha CMR, Goncalves MP (2020) Chapter 24- agar. In: Phillips GO, Williams PA (eds) Handbook of hydrocolloids, 3rd edn. Woodhead Publishing Elsevier, Sawston, pp 731–765
28. Song E-H, Shang H, Ratner DM (2012) 9.08 - Polysaccharides. In: Matyjaszewski K, Möller M (eds) Polymer science: a comprehensive reference, vol 9, 1st edn. Elsevier Science, Amsterdam, pp 137–55
29. Ayyad O, Muñoz-Rojas D, Agulló N, Borrós S, Gómez-Romero P (2010) High-concentration compact agar gels from hydrothermal synthesis. Soft Matter 6(11):2389–2391
30. Brown ZK, Fryer PJ, Norton IT, Bridson RH (2010) Drying of agar gels using supercritical carbon dioxide. J Supercrit Fluids 54(1):89–95
31. Guastaferro M, Baldino L, Reverchon E, Cardea S (2021) Production of porous agarose-based structures: freeze-drying vs. supercritical CO2 drying. Gels 7:198
32. Athamneh T, Hajnal A, Al-Najjar MAA, Alshweiat A, Obeidat R, Awad AA et al (2023) In vivo tests of a novel wound dressing based on agar aerogel. Int J Biol Macromol 239:124238
33. Basak S, Singhal RS (2023) The potential of supercritical drying as a "green" method for the production of food-grade bioaerogels: a comprehensive critical review. Food Hydrocoll 141:108738
34. Agar MT (1990). In: Harris P (ed) Food gels, 1st edn. Springer, Dordrecht, pp 1–51
35. Gurikov P, Raman SP, Weinrich D, Fricke M, Smirnova I (2015) A novel approach to alginate aerogels: carbon dioxide induced gelation. RSC Adv 5(11):7812–7818
36. Keil C, Hübner C, Richter C, Lier S, Barthel L, Meyer V et al (2020) Ca-Zn-Ag alginate aerogels for wound healing applications: swelling behavior in simulated human body fluids and effect on macrophages. Polymers (Basel) 12(11):1–17
37. EDANA. Free Swell Capacity, No NWSP 240.0.R2 (19) (2019) Harmonized nonwovens standard procedures: polyacrylate superabsorbent powders-determination of the free swell capacity in saline by gravimetric measurement. Brussels, Belgium
38. Raman SP, Keil C, Dieringer P, Hübner C, Bueno A, Gurikov P et al (2019) Alginate aerogels carrying calcium, zinc and silver cations for wound care: fabrication and metal detection. J Supercrit Fluids 153:104545

39. EDANA/INDA. Centrifuge retention capacity, No NWSP 241.0.R2 (19) (2019) Harmonized nonwovens standard procedures: polyacrylate superabsorbent powders-determination of the fluid retention capacity in saline solution by gravimetric measurement following centrifugation. Brussels, Belgium
40. Aaronson SA, Todaro GJ (1968) Development of 3T3-like lines from Balb-c mouse embryo cultures: transformation susceptibility to SV40. J Cell Physiol 72(2):141–148
41. Boukamp P, Petrussevska RT, Breitkreutz D, Hornung J, Markham A, Fusenig NE (1988) Normal keratinization in a spontaneously immortalized aneuploid human keratinocyte cell line. J Cell Biol 106(3):761–771
42. Tsuchiya S, Yamabe M, Yamaguchi Y, Kobayashi Y, Konno T, Tada K (1980) Establishment and characterization of a human acute monocytic leukemia cell line (THP-1). Int J Cancer 26:171–176. https://doi.org/10.1002/ijc.2910260208
43. Maares M, Keil C, Thomsen S, Günzel D, Wiesner B, Haase H (2018) Characterization of Caco-2 cells stably expressing the protein-based zinc probe eCalwy-5 as a model system for investigating intestinal zinc transport. J Trace Elem Med Biol 49:296–304
44. Kamiloglu S, Sari G, Ozdal T, Capanoglu E (2020) Guidelines for cell viability assays. Food Front 1(3):332–349
45. Lund ME, To J, O'Brien BA, Donnelly S (2016) The choice of phorbol 12-myristate 13-acetate differentiation protocol influences the response of THP-1 macrophages to a pro-inflammatory stimulus. J Immunol Methods 430:64–70
46. Narayanan J, Xiong JY, Liu XY (2006) Determination of agarose gel pore size: absorbance measurements vis a vis other techniques. J Phys Conf Ser 28(1):83–86
47. Rege A, Aney S, Milow B (2021) Influence of pore-size distributions and pore-wall mechanics on the mechanical behavior of cellular solids like aerogels. Phys Rev E [Internet] 103(4):43001. https://doi.org/10.1103/PhysRevE.103.043001
48. Chandrasekaran R, Hillgärtner M, Ganesan K, Milow B, Itskov M, Rege A (2021) Computational design of biopolymer aerogels and predictive modelling of their nanostructure and mechanical behaviour. Sci Rep 11(1):1–10
49. Robitzer M, Tourrette A, Horga R, Valentin R, Boissire M, Devoisselle JM et al (2011) Nitrogen sorption as a tool for the characterisation of polysaccharide aerogels. Carbohydr Polym 85(1):44–53
50. Kumar S, Boro JC, Ray D, Mukherjee A, Dutta J (2019) Bionanocomposite films of agar incorporated with ZnO nanoparticles as an active packaging material for shelf life extension of green grape. Heliyon 5(6):e01867
51. Murdock JN, Wetzel DL (2009) FT-IR microspectroscopy enhances biological and ecological analysis of algae. Appl Spectrosc Rev 44(4):335–361
52. Pereira L, Gheda SF, Ribeiro-Claro PJA (2013) Analysis by vibrational spectroscopy of seaweed polysaccharides with potential use in food, pharmaceutical, and cosmetic industries. Int J Carbohydr Chem 2013:1–7
53. Mißfeldt F, Gurikov P, Lölsberg W, Weinrich D, Lied F, Fricke M et al (2020) Continuous supercritical drying of aerogel particles: proof of concept. Ind Eng Chem Res 59(24):11284–11295
54. Valentin R, Horga R, Bonelli B, Garrone E, Di Renzo F, Quignard F (2006) FTIR spectroscopy of NH3 on acidic and ionotropic alginate aerogels. Biomacromol 7(3):877–882
55. Horga R, Di Renzo F, Quignard F (2007) Ionotropic alginate aerogels as precursors of dispersed oxide phases. Appl Catal A Gen 325(2):251–255
56. Paraskevopoulou P, Smirnova I, Athamneh T, Papastergiou M, Chriti D, Mali G et al (2020) Mechanically strong polyurea/polyurethane-cross-linked alginate aerogels. ACS Appl Polym Mater 2(5):1974–1988
57. Paraskevopoulou P, Smirnova I, Athamneh T, Papastergiou M, Chriti D, Mali G et al (2020) Polyurea-crosslinked biopolymer aerogel beads. RSC Adv 10(67):40843–40852
58. Rostamitabar M, Subrahmanyam R, Gurikov P, Seide G, Jockenhoevel S, Ghazanfari S (2021) Cellulose aerogel micro fibers for drug delivery applications. Mater Sci Eng C 127:112196
59. Xu N, Zhang X, Qi T, Wu Y, Xie X, Chen F et al (2022) Biomedical applications and prospects of temperature-orchestrated photothermal therapy. MedComm Biomater Appl 1(2):25
60. Gu Y, Mu X, Wang P, Wang X, Liu J, Shi J et al (2020) Integrated photothermal aerogels with ultrahigh-performance solar steam generation. Nano Energy [Internet] 74:104857. https://doi.org/10.1016/j.nanoen.2020.104857
61. Zhang X, Tan B, Wu Y, Zhang M, Liao J (2021) A review on hydrogels with photothermal effect in wound healing and bone tissue engineering. Polymers (Basel) 13(13):2100

62. Nguyen HG, Nguyen TAH, Do DB, Pham XN, Nguyen TH, Nghiem HLT et al (2023) Natural cellulose fiber-derived photothermal aerogel for efficient and sustainable solar desalination. Langmuir 39(19):6780–6793
63. Shah R, Saha N, Saha P (2015) Influence of temperature, pH and simulated biological solutions on swelling and structural properties of biomineralized (CaCO3) PVP–CMC hydrogel. Prog Biomater 4(2–4):123–136
64. Forgács A, Papp V, Paul G, Marchese L, Len A, Dudás Z et al (2021) Mechanism of hydration and hydration induced structural changes of calcium alginate aerogel. ACS Appl Mater Interfaces 13(2):2997–3010
65. Holt RM, Glass RJ, Sigda JM, Mattson ED (2003) Influence of centrifugal forces on phase structure in partially saturated media. Geophys Res Lett 30(13):3–6
66. Schaudinn C, Dittmann C, Jurisch J, Laue M, Günday-Türeli N, Blume-Peytavi U et al (2017) Development, standardization and testing of a bacterial wound infection model based on ex vivo human skin. PLoS ONE 12(11):1–13
67. Rancan F, Jurisch J, Hadam S, Vogt A, Blume-Peytavi U, Bayer IS et al (2023) Ciprofloxacin-loaded polyvinylpyrrolidone foils for the topical treatment of wound infections with methicillin-resistant staphylococcus aureus (MRSA). Pharmaceutics 15(7):1876